

20742.

^(b)Max Kade Fellow on leave from Technische Universität, München, West Germany.

^(c)Present address: Applied Mathematics Division, Argonne National Laboratory, Argonne, Ill. 60439.

¹H. E. Jackson *et al.*, Phys. Rev. C **16**, 730 (1977).

²C. A. Goulding and J. G. Rogers, TRIUMF Report No. TRI-75-3 (unpublished).

³C. Richard-Serre *et al.*, Nucl. Phys. **20B**, 413 (1970); and B. M. Preedom *et al.*, Phys. Lett. **65B**, 31 (1976).

⁴C. Lovelace *et al.*, Lawrence Berkeley Laboratory Report No. LBL-63, 1973 (unpublished).

Anomalous Optical-Model Potential for Sub-Coulomb Protons for $89 < A < 130$

C. H. Johnson

Oak Ridge National Laboratory, Oak Ridge, Tennessee 37830

and

A. Galonsky

Michigan State University, East Lansing, Michigan 48824

and

R. L. Kernell

Old Dominion University, Norfolk, Virginia 23506

(Received 3 October 1977)

The (p, n) cross sections for fourteen nuclei from $A = 89$ to $A = 130$ were measured from about 2.5 to 5.8 MeV in order to obtain total reaction cross sections. These cross sections disagree with optical-model predictions in that the predicted $3p$ resonance is missing near $A = 105$ and the peak near $A = 90$ is replaced by a valley. The data can be described by introducing an anomalous A dependence into the depth of the absorptive potential.

We present arguments with supporting data that certain experiments should be exploited to learn more about the optical-model potential (OMP) for protons. The experiments are to measure (p, n) cross sections for protons incident below the Coulomb barrier. Data from initial experiments of this type show that the OMP for $89 < A < 130$ has an anomalous behavior which merits more study.

A strength function $\langle \gamma_{lJ}^2 \rangle / \langle D_{lJ} \rangle$ is the ratio of the reduced particle width to level spacing averaged over the closely spaced compound-nuclear states of spin J formed by l -wave particles. Our contribution deals with protons, but first we comment on the familiar neutron strength functions.¹ Neutron single-particle states give rise to giant "size" resonances that are observed in plots of the strength function versus mass number for s waves near $A = 55$ and 160 and for p waves near $A = 95$. One can describe the resonances approximately by the OMP by "tuning" the volume of the real well to fit the resonant masses and by adjusting the imaginary part and the diffuseness to give the height and width of each resonance. As for the $A = 160$ resonance, the $3p$ resonance near $= 95$ may be split. Although a splitting was at-

tributed to vibrational motions,² the early-found strength-function data have been questioned,¹ and recent precision total-cross-section measurements suggest that the resonance is smooth and without structure.³

We would like to emphasize the complementary information on the nucleon OMP to be obtained from protons incident below the Coulomb barrier. There is a dearth of precision sub-Coulomb data, perhaps because workers recognize the barrier's problems more than its benefits. There are problems. Resonances are difficult to resolve because the energies needed for barrier penetration are much larger than the level spacings. Even so, Bilpuch *et al.*⁴ obtained strength functions by resolving resonances for $A < 65$. For higher masses for which individual levels cannot be resolved, useful data can be obtained if the average energies and cross sections are measured accurately and the Coulomb penetrabilities are divided out to reveal the nuclear effects.

The Coulomb barrier has two beneficial effects. The first, which seems not to be fully appreciated, is that the barrier, by virtue of its height relative to the spreading width from the absorptive potential, can quasibind a single-particle

state. Thus, we anticipate that a single-particle resonance may be sharpened sufficiently to be observed as a function of proton energy for a given nucleus. The picture then has three dimensions rather than only two, as for neutrons. Collective and shell effects might then be revealed as we move from one nucleus to the next. The second benefit is experimental and long recognized, viz., for energies well above the (p, n) threshold but below the Coulomb barrier the energy-averaged total (p, n) cross section $\langle\sigma_{p,n}\rangle$, which is relatively easy to measure, is nearly the entire total reaction cross section $\langle\sigma_r\rangle$. The conversion of $\langle\sigma_{p,n}\rangle$ to $\langle\sigma_r\rangle$ usually requires only a small correction for γ -ray emission, and that can be made using known radiation strengths from neutron capture. Corrections for proton reemission are

small.

The proton $3p$ resonance was found in five Sn isotopes^{5,6} by this technique. Figure 1(a) shows OMP fits⁶ to those Sn data plus predictions for other nuclei from $A = 89$ to $A = 130$. Plotted vertically are the reduced proton total reaction cross sections defined by^{6,7}

$$\langle S_p \rangle = \langle \sigma_r \rangle / [4\pi^2 k^{-1} \sum_l (2l+1) A_l^{-2}] \quad (1)$$

where A_l^{-2} is a usual sum of squared Coulomb wave functions. This $\langle S_p \rangle$ is essentially^{6,7} the l -wave-weighted average of proton strength functions. The corresponding reduced (p, n) cross section $\langle S_{p,n} \rangle$ is found by replacing $\langle \sigma_r \rangle$ by $\langle \sigma_{p,n} \rangle$ in (1).

The OMP used was a conventional sum of Woods-Saxon, surface absorptive, spin-orbit, and Coulomb potentials:

$$V(r) = -V_R f(r, R_R, a_R) + i4a_D W_D \frac{d}{dr} f(r, R_D, a_D) + V_{s.o.} \frac{\vec{\sigma} \cdot \vec{r}}{r} \left(\frac{\hbar}{m_\pi c} \right)^2 \frac{d}{dr} f(r, R_{s.o.}, a_{s.o.}) + V_C(R_C), \quad (2)$$

where

$$f(r, R, a) = \{1 + \exp[(r - R)/a]\}^{-1},$$

$$R_x = r_x A^{1/3},$$

$$V_R(E) = V_R(0) - b_0 E,$$

and $V_C(R_C)$ is the potential for a uniformly charged sphere. This potential, which has been developed in the literature by analyses of differential, polarization, and reaction cross sections for protons above the Coulomb barrier, has more parameters than needed for the sub-Coulomb data. Only three free parameters are needed to fit the energy, height, and width of an observed resonance in the strength function. An extensive study⁶ of parameter space showed that a_D , W_D , and $V_R(0)$ were appropriate free parameters. Thus, these three were adjusted by least squares while the others were fixed according to published analyses of data obtained above the barrier.

That extensive analysis⁶ for the Sn (p, n) cross sections is an essential anchor for the present work. To predict the other curves in Fig. 1(a) we used the same OMP as for Sn (specifically for ¹¹⁷Sn) except for slight variations in $V_R(0)$ according to a conventional isospin and Coulomb dependence,⁸

$$V_R(0) = V_0 + 24(N - Z)/A + 0.45 Z/A^{1/3},$$

$$V_0 = 55.4 \text{ MeV} \quad (3)$$

This expression predicts an A dependence for the

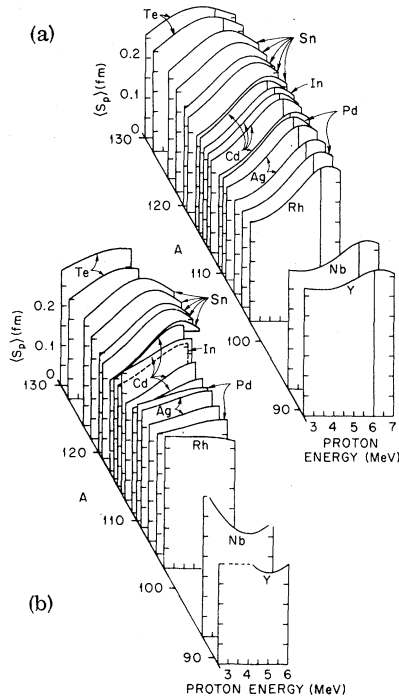


FIG. 1. Excitation functions for reduced proton total reaction cross sections for nuclei from $A = 89$ to 130. (a) Predicted. The required optical-model parameters were derived from fits to data on the five Sn isotopes, as shown (see Ref. 6). The vertical lines at 6 MeV aid in visual comparisons to (b). (b) Observed. For clarity of presentation, well-fitted curves rather than data are shown. See Fig. 2 for a representative fit to data. The nuclei are the same as in (a).

isotopes of a given element; however, since negligible dependence was observed⁶ for Sn, we assumed N and A from the minimum in the valley of β stability for calculating $V_R(0)$ for all isotopes of each element. The variation of $V_R(0)$ for the nuclei in Fig. 1(a) is only 1.7 MeV. We see that the predicted peak moves from 6.3 MeV for ^{89}Y to 5.3 MeV for ^{130}Te . This slow decrease demonstrates the nearly compensating effects of the increasing volume of the real nuclear well and the increasing repulsion of the Coulomb potential.

To test these predictions, we have analyzed published^{5,9} $\langle\sigma_{p,n}\rangle$ for ^{89}Y and In and unpublished¹⁰ data for ^{93}Nb , ^{103}Rh , $^{105,110}\text{Pd}$, $^{107,109}\text{Ag}$, $^{111,113,114,116}\text{Cd}$, and $^{128,130}\text{Te}$. All were measured some time ago using the same accelerator and absolute 4π neutron detector as for the Sn data. The targets were of such thickness, typically 50 keV, that the cross sections represent averages over many compound states. The observed isobaric analog resonances were omitted from the subsequent analysis. Although a few excitation functions show some erratic behavior due to nonuniformities and trace impurities of light elements, we believe that there are no overall systematic errors. Thus, we can compare the general pattern to the predictions.

To illustrate, we present in Fig. 2 data and curves for ^{109}Ag . The dashed curve is the prediction from Fig. 1(a). The lower solid curve shows $\langle S_{p,n}\rangle$ obtained by least-squares adjustment of only W_D and a_D for the absorptive potential, and the upper solid curve is the corresponding $\langle S_p\rangle$. [The small difference is caused by the (p,γ) process which we calculated using neutron radiative cap-

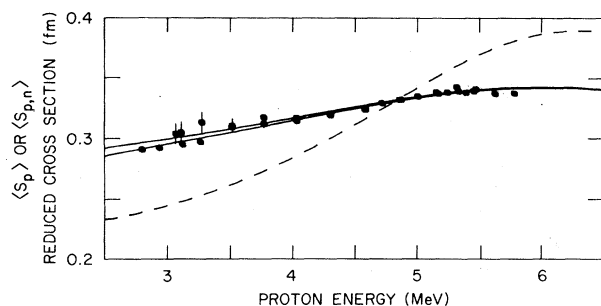


FIG. 2. Reduced proton cross sections for ^{109}Ag . The dashed curve is the $\langle S_p\rangle$ prediction from Fig. 1(a). Data points are the reduced (p,n) cross sections, $\langle S_{p,n}\rangle$. The lower solid curve is $\langle S_{p,n}\rangle$ found by least-squares adjustment of W_D and a_D with the other model parameters as in the dashed curve. The upper curve is the corresponding $\langle S_p\rangle$.

ture data and the statistical model.] The predicted and observed excitation functions are in considerable disagreement.

In a similar manner we analyzed the other excitation functions. For $A > 100$ each fit gave nearly the same diffuseness, $a_D \approx 0.4$ fm. For ^{89}Y and ^{93}Nb , however, the searches did not converge to good fits with $V_R(0)$ fixed by Eq. (3); therefore, we fixed a_D at 0.4 fm and varied W_D and V_0 . Figure 1(b) shows the best-fit curves along with the Sn curves from Fig. 1(a).

Below $A = 116$ the predicted curves [Fig. 1(a)] are quite different from the experimental curves [Fig. 1(b)]. We attribute the fluctuations in average height from one nucleus to the next to uncertainties in target densities. The largest fluctuation is for ^{114}Cd ; its curve averages about 15% above its neighbors. The significant fact, however, is that the shapes of the curves change progressively from the predictions for nuclei lighter than Sn. For ^{103}Rh the predicted peak is missing, and near $A = 90$ it is replaced by a valley. In the above fitting with the OMP this trend is described by a systematic variation in the strength W_D of the absorptive potential, as shown in Fig. 3. The curve, which is drawn visually, has a maximum near $A = 105$ and may have minima near $A = 90$ and 120. (The very large W_D for ^{103}Rh has a large uncertainty; essentially it represents a black nucleus.)

These data could be described by variations in parameters other than W_D ; our studies indicate

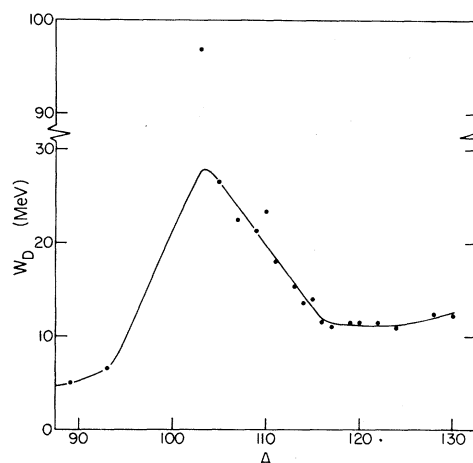


FIG. 3. Absorptive well depths for the fitted curves of Fig. 1(b). For $A > 100$ the corresponding least-squares-fitted values of a_D were all about 0.4 fm. For $A < 100$, a_D was set equal to 0.4 fm, and V_0 and W_D were searched on. The curve is drawn visually.

that we could vary b_0 drastically with corresponding adjustments in $V_R(0)$. But we find no way to describe these data in the true spirit of the OMP, i.e., with all parameters having only slight and monotonic dependences on N , Z , and A .

At present the explanation for these variations is not clear. Perhaps they result from the vibrational effects which are particularly strong¹¹ near $A = 105$. However, vibrational effects should show structure other than the observed smooth A dependence. In particular, the ¹¹⁶Cd nucleus, which is more deformable than the Sn isotopes, should show a flattened resonance rather than the observed strong resonance similar to the neighboring Sn nuclei.

Possibly we are observing the shell effects proposed by Lane *et al.*¹² and Lynn¹ to explain anomalies in the neutron strength functions in this mass region. Near closed shells the low density of two-particle, one-hole states available to the incident particle is expected to reduce the absorptive strength W_D . Thus, in Fig. 3 the small W_D near $A = 120$ may result from the fifty-proton shell and the even lower W_D near $A = 90$ may result from the fifty-neutron shell.

We urge that measurements of the type reported here be extended over a larger region of mass and energy. It would be of particular interest to extend the data to higher energies to locate the resonance peaks and to include higher and lower

masses to see if W_D truly has minima at the fifty-nucleon shells. The facility for the present work is no longer available.

This research was sponsored by U. S. Energy Research and Development Administration under contract with Union Carbide Corporation and by the National Science Foundation.

¹J. E. Lynn, *Theory of Neutron Resonance Relations* (Clarendon, Oxford, England, 1968).

²B. Buck and F. Perey, *Phys. Rev. Lett.* **8**, 444 (1962).

³H. S. Camarda, *Phys. Rev. C* **9**, 28 (1974).

⁴E. G. Bilpuch, A. M. Lane, G. E. Mitchell, and J. D. Moses, *Phys. Rep.* **28C**, 145 (1976).

⁵C. H. Johnson and R. L. Kernell, *Phys. Rev. C* **2**, 639 (1970).

⁶C. H. Johnson, J. K. Bair, C. M. Jones, S. K. Penny, and D. W. Smith, *Phys. Rev. C* **15**, 196 (1977).

⁷J. P. Schiffer and L. L. Lee, Jr., *Phys. Rev.* **109**, 2098 (1958).

⁸F. D. Becchetti and G. W. Greenlees, *Phys. Rev.* **182**, 1190 (1969).

⁹C. H. Johnson, R. L. Kernell, and S. Ramavataram, *Nucl. Phys.* **A107**, 21 (1968).

¹⁰C. H. Johnson, A. Galonsky, and C. H. Inskeep, Oak Ridge National Laboratory Report No. ORNL-2910, 1960 (unpublished).

¹¹P. H. Stelson and L. Grodzins, *Nucl. Data, Sect. A* **1**, 21 (1965).

¹²A. M. Lane, J. E. Lynn, E. Melkonian, and E. R. Rae, *Phys. Rev. Lett.* **2**, 424 (1959).